NUMERICAL STUDY OF DYNAMIC LOADING IN EX-PORO-HYDRODYNAMIC LUBRICATION. 3D CASE STUDY: HUMAN FOOTPRINT IMPACT OVER A HIGHLY COMPRESSIBLE POROUS LAYER SATURATED WITH WATER

Cristian S. POPESCU[1]

Studii teoretice şi experimentale recente desfăşurate în lubrificaţia ex-poro-hidrodinamică subliniază capacitatea unui strat poros extrem de compresibil (SPEC), saturat complet cu un lichid newtonian, de a disipa energia unui impact. Au fost elaborate modele analitice pentru configuraţii simple, cum ar fi expulzarea lichidului din SPEC între plăci paralele sau la impactul unei sfere, care se bazează pe variaţia permeabilităţii dată de relaţia Kozeny-Carman, în funcţie de porozitate/compactitate. Considerând diverse aplicaţii posibile, această lucrare introduce modelarea numerică (metoda volumului finit) a expulzării lichidului din SPEC la viteză constantă (validată de experiment), la forţă constantă şi sub impact.

Recent theoretical and experimental studies performed in ex-poro-hydrodynamic lubrication underline the ability of a highly compressible porous layer (HCPL), completely saturated with a Newtonian liquid, to dissipate the energy of an impact. Analytical models were developed for simple configurations, such as HCPL squeezed between parallel plates or by a sphere, that are based on the permeability variation given by Kozeny-Carman equation, as function of porosity/compacticity. Considering possible future applications, this paper introduces the numerical modeling (finite volume method) of the liquid squeezed from a HCPL at constant velocity (validated by experiment), at constant force and under impact.

Keywords: squeeze, impact, porous, deformable, dynamic permeability, CFD

1. Introduction

Recent theoretical and experimental work performed in ex-poro-hydrodynamic lubrication (XPHDL) underlines the ability of a highly compressible porous layer (HCPL), completely saturated with a Newtonian liquid, to dissipate the energy of a squeeze/impact [1-7]. Taking into account the local deformation of a HCPL, the hydrodynamic forces generated in the internal structure of the HCPL allow, within certain limits, the total absorption of the

[1] PhD, Depart. of Machine and Tribology, University POLITEHNICA of Bucharest, Romania, e-mail: cristiansorinpopescu@yahoo.com

energy of a squeeze/impact. The same phenomenon is under research at City University of New-York, for random soft porous media that generate lift forces to self sustain carried loads, under a sliding motion [8-11].

Porous materials that can be included in the HCPL category are: the endothelial surface glycocalyx [5 and 12], the fresh powder snow [8], the goose down [9], the articular cartilage [13], also woven and unwoven textile materials, such as felt or wash-cloth [1,4,14 and 15].

Theoretical models take into consideration material properties of the liquid and of the HCPL and are based on the permeability variation of the porous media, as function of its porosity/compacticity [16], given by Kozeny-Carman equation [16 and 17]. The permeability was determined in stationary conditions [14] but the dynamic processes considered in all configurations of XPHDL have a direct influence on the permeability variation of the HCPL, therefore recent studies were performed on unwoven textile materials to determine the variation of the dynamic permeability of a HCPL under dynamic loading [15].

The theoretical modeling in XPHDL of the HCPL completely saturated with Newtonian liquid, under squeeze at constant velocity and under impact was focused on analytical models developed for simple configurations [1-7]. The HCPL placed on a fixed rigid support is squeezed by a rigid body, such as a plate (circular or rectangular) that is parallel with the fixed rigid support, or a free-falling sphere. The thickness/compacticity is imposed by the body-shaped-function of the impactor, therefore at a certain moment the thickness can be uniform (in the case of parallel plates) or non-uniform (in the case of the sphere).

Considering the great number of possible applications working at atmospheric pressure as open systems (porous coating, viscosity pump) or under pressure as closed systems (shock absorber, squeeze film damper), this paper introduces a numerical modeling (performed with the commercial software Ansys Fluent) of the squeeze at constant velocity / at constant loading / under impact of a HCPL, completely saturated with a Newtonian liquid, that allows the approach of diverse configurations with various body-shapes.

2. Theoretical model

The general configuration of the normal squeeze of the HCPL completely saturated with a Newtonian liquid placed between a moving rigid body of mass M and a fixed rigid support is presented in Fig.1.

The HCPL is considered as isotropic material, its permeability variation as function of compacticity being given by Kozeny-Carman function [17]:

$$\phi = D\frac{(1-\sigma)^3}{\sigma^2} \tag{1}$$

where $D = d^2/16k$ is the complex parameter, with d the diameter of the fibre and k a correction constant.

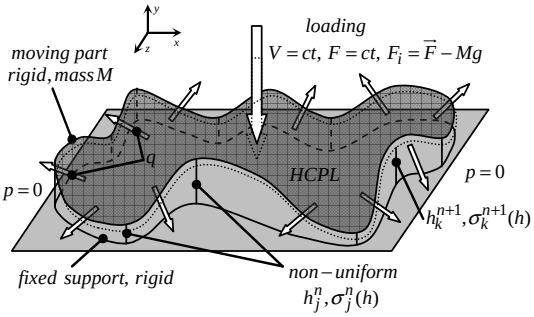

Fig. 1. The general configuration of the normal squeeze of the HCPL completely saturated with Newtonian liquid.

The compacticity of HCPL is determined as function of its thickness and in terms of the initial thickness and the initial compacticity [2]:

$$\sigma = \frac{\sigma_0 h_0}{h} \tag{2}$$

The dynamic property of the permeability is given by the variable complex parameter D, initially used as a constant, its functions being approximated from experiments performed on HCPL squeezed under impact or at constant velocity [15]:

$$\begin{aligned} D_{compr}^{imp} &= \frac{d_1^2}{16k_1}(0.145 - 0.343H_m + 0.282H_m^2) \\ D_{decompr}^{imp} &= \frac{d_1^2}{16k_1}(0.077 - 0.315H_m + 0.355H_m^2) \end{aligned} \tag{3}$$

where $d_1 \approx 18\mu m$ is the average fibre diameter of material M1, $k_1 = 5$ the determined correction constant, configuration sphere+M1+water;

$$D_{compr}^{v=ct} = \frac{d_2^2}{16k_2}(2.21 - 8.68H + 10.251H^2) \tag{4}$$

and $d_2 \approx 12\mu m$ is the average fibre diameter of material M2, $k_2 = 0.18\text{K } 0.2$ the determined correction constant, configuration disc+M2+oil.

Considering the dynamic configuration involved, the uniform / non-uniform thickness of the HCPL is modified at each time step and so are the parameters depending on it: compacticity and permeability. The numerical solutions are provided by solving the Navier-Stokes system of equations coupled with the continuity equation, implemented in the solver of the commercial software Ansys-Fluent [18]. When the inertial loss term is neglected, the

momentum equations for porous media are reduced to Darcy's law. The numerical solutions are computed by the Finite Volume Method with the pressure-based solver that provides fluid dynamics within a porous material with variable compacticity/permeability, and with the Six Degree of Freedom solver (6DOF) for the solid-body kinematics.

3. Validation of the model

The first validation of the presented model consists in the comparison of the numerical results with the experimental data and the analytical solutions in the case of squeeze at constant velocity of a HCPL saturated with liquid.

The experimental data was determined for the squeeze configuration disc+HCPL+liquid [15], and the force analytically obtained [3], is:

$$F = \frac{\pi}{8} \cdot \frac{\eta R^4 V}{D} \cdot \frac{\sigma_0^2 h_0^2}{h(h-\sigma_0 h_0)^2} \tag{5}$$

The results for the squeeze at constant velocity, configuration disc+M2+SAE20W50 oil, are presented in Fig.2. A very good correspondence is observed between the experiment and the numerical results, therefore the model is considered validated for squeeze at constant velocity.

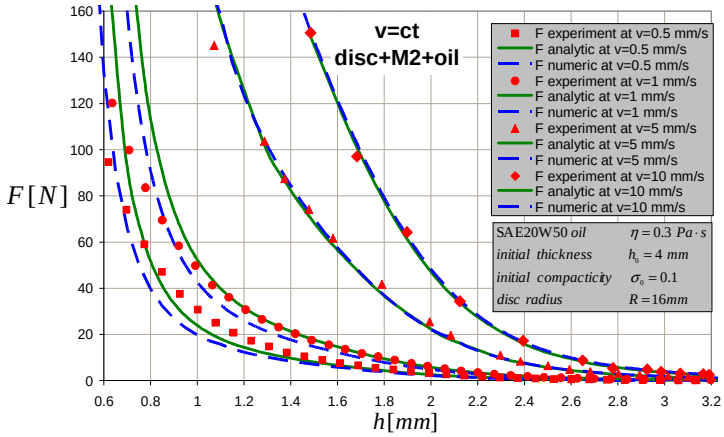

Fig. 2. Comparison of force vs. thickness between experimental data, analytical model and numerical results for squeeze at constant velocity, disc+M2+oil.

In the case of HCPL impacted by a rigid, the numerical results are compared with the analytical solutions. The impact force and the velocity are obtained from the analytical model of the impact of a circular plate over a HCPL, in restrained conditions [6]:

$$F = \frac{\pi \eta \sigma_0^2 R^4}{8D h_0 H (H-\sigma_0)^2}\left[V_0 - \frac{\pi \eta R^4}{8DM}\left(\ln\frac{H-\sigma_0}{H(1-\sigma_0)} + \frac{\sigma_0(1-H)}{(H-\sigma_0)(1-\sigma_0)}\right)\right]$$
$$V = V_0 - \frac{\pi \eta R^4}{8DM}\left(\ln\frac{H-\sigma_0}{H(1-\sigma_0)} + \frac{\sigma_0(1-H)}{(H-\sigma_0)(1-\sigma_0)}\right) \quad (6)$$

The results presented in Fig.3 were obtained for the impact configuration disc+M1+water, with discs having the same initial velocity $V_0 = 1\, m/s$ but different masses: $M = 0.1; 1; 10\, kg$. In each case the comparison of force is performed with respect to the maximum force obtained from the analytical model (Eq.6). The extreme weights were chosen mainly to test the thickness response of M1 impacted by a rigid disc.

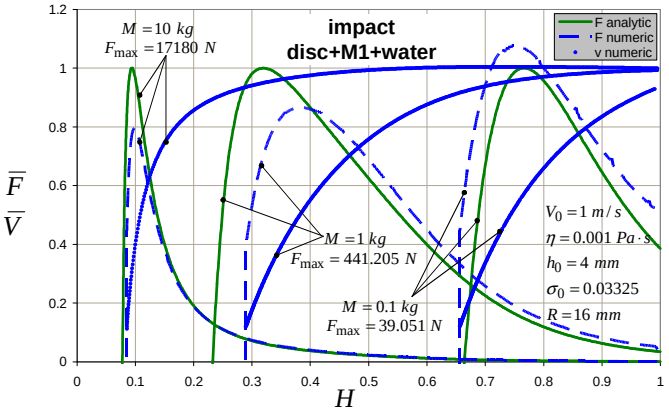

Fig. 3. Comparison of the normalized force and velocity vs. dimensionless thickness between analytical model and numerical results for impact, disc+M1+water.

Although the comparison from Fig.3 shows a good correspondence between the two models, the results are not reliable because the thickness of M1 should drastically decrease by increasing the mass of the disc. Considering that the contact area between the disc and M1 is constant and the area where the flow takes place is influenced not only by the initial velocity of the disc but also by its mass, a correction has to be made to the permeability variation. Therefore, assuming that the permeability variation has the same trend for any impact (reflected from the constant velocity experiment), it is shifted depending on the mass and the initial velocity of the impactor. Starting from the impact experiment, taking into consideration the velocity ($2.35\, m/s$) and the mass ($13.53\, g$) of the impactor, rearranging the terms, one obtains the complex parameter:

$$D_{compr}^{imp} = \frac{d_1^2}{16}\,\overline{p}_0\,(0.912 - 2.157\,H + 1.774\,H^2)$$
$$D_{decompr}^{imp} = \frac{d_1^2}{16}\,\overline{p}_0\,(0.484 - 1.981\,H + 2.233\,H^2) \tag{7}$$

where the initial dimensionless momentum $\overline{p}_0 = \overline{M}\,\overline{V}_0$ carries the impact information to the permeability variation.

The permeability variations computed with the complex parameters obtained from Eqs. 3 and 7 are used to plot the force vs. thickness, Fig.4, in the impact case of disc+M1+water, when the disc has an initial velocity of $1\,m/s$ and a mass of $1\,kg$, in the compression stage. A reliable result is obtained when Eq.7 with $\overline{p}_0 = \overline{M}\,\overline{V}_0 = 1$ is used.

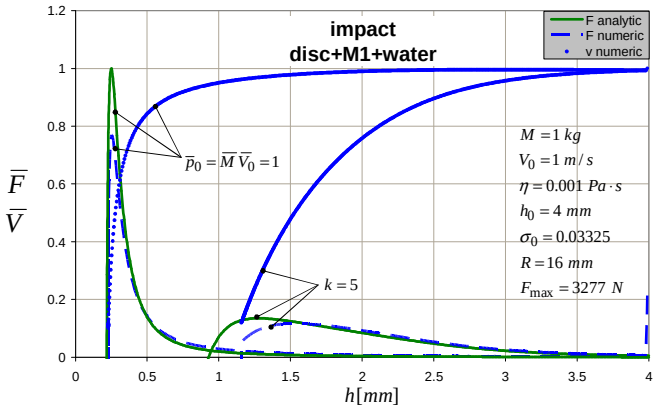

Fig. 4. Comparison of the normalized force and velocity vs. thickness between analytical model and numerical results for impact when material constant is influenced by the velocity and the mass, disc+M1+water.

4. Results and discussion

A constant loading was applied to the disc on a normal direction in order to observe the response of the HCPL saturated with a Newtonian liquid, using the dynamic permeability determined from the constant velocity test. The numerical results obtained for the configuration disc+M2+oil are shown in Fig.5.

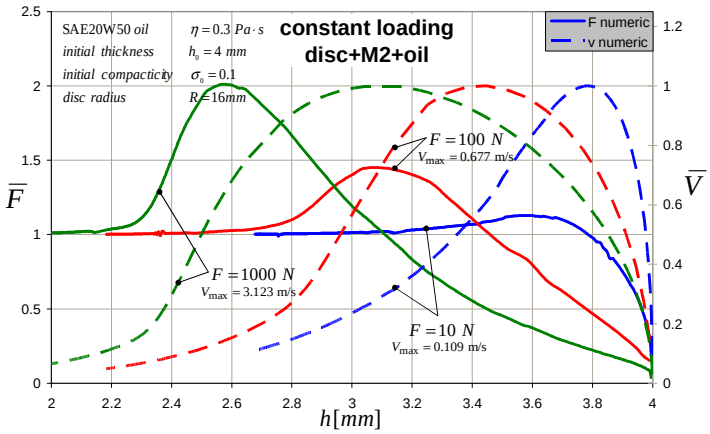

Fig. 5. Comparison of the normalized force and velocity vs. thickness between analytical model and numerical results for impact when material constant is influenced by the velocity and the mass, disc+M1+water.

For each case the force is normalized by the constant applied value, respectively $10\ N$, $100\ N$, $1000\ N$ and the velocity is normalized with the maximum velocity reached by the disc.

This particular case emphasizes the hydrodynamic forces generated by the HCPL under loading. The three stages of the test are given by the coupled variations of the velocity and the force. In the first stage the disc with no initial velocity starts to generate pressure on the HCPL, which reacts by increasing the force. The second stage starts when the disc has reached a maximum velocity. At this point, the force has about the same value as the one imposed by the constant loading. Although the disc has decreasing velocity, the HCPL still responds by increasing the force until a maximum force is achieved. In the third stage, the velocity of the disc is decreased until small values are reached, along with the force that is no longer influenced by the HCPL and keeps the constant value imposed.

For the impact configuration, a particular and relevant situation occurs when the initial dimensionless momentum $\overline{p}_0 = \overline{M} \cdot \overline{V}_0$ takes the same value for two different cases. An example was chosen for the impact configuration (disc+M1+water) with $\overline{p}_0 = 0.5$: a mass of $0.5\ kg$ with an initial velocity of $1\ m/s$, respectively a mass of $1\ kg$ with an initial velocity of $0.5\ m/s$.

In one case from Fig.6 there is a very good correspondence between the two models but, for the other case, there is a significant difference in the force values (almost doubled), which can be explained by a velocity over estimated by the analytical model. One can also remark that the velocity of $0.5\ m/s$, applied to the disc with mass of $1\ kg$, is slowly increased up to a maximum value in the

numerical simulation due to the gravitational acceleration and a weak response of the HCPL.

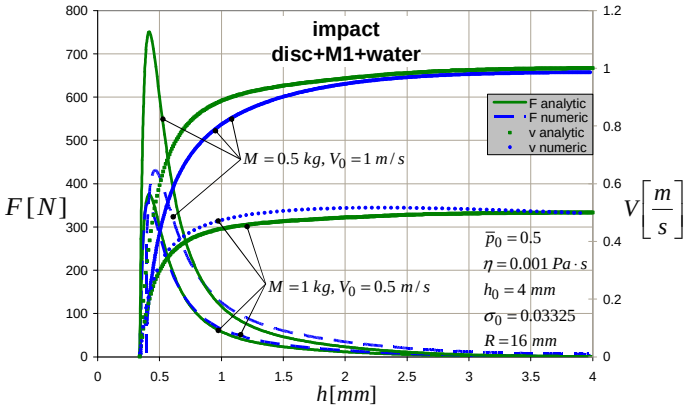

Fig. 6. Comparison of the force and the velocity vs. thickness between analytical model and numerical results for impact when $\bar{p}_0 = 0.5$, disc+M1+water.

The thickness variation of a HCPL under impact is also important. Therefore, another example is shown in Fig.7 for the impact configuration disc+M1+water, introducing the thickness besides force and velocity. The dimensionless functions (thickness as function of time, force and velocity with respect to thickness) are represented when different initial velocities are applied to the rigid disc with a mass of $0.5\ kg$.

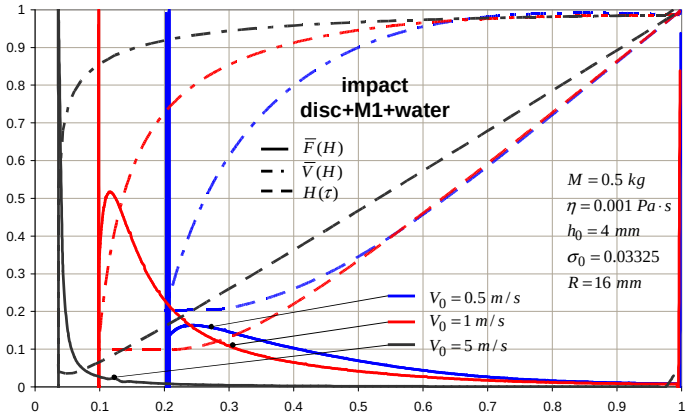

Fig. 7. Numerical results for the impact of a rigid disc with different initial velocities over a HCPL saturated with Newtonian liquid. Force, velocity and thickness for the impact configuration disc+M1+water.

The direct influence of the velocity upon the thickness of the HCPL can be observed when different initial velocities are given to a disc with the same mass, Fig.7. The velocity of the disc is continuously decreased and the thickness of the HCPL reaches a minimum value when the velocity becomes zero. An inflexion is

remarked in the force variation, before the end of the impact, followed by a strong response of the HCPL when the total energy of the impact is dissipated. In the case with the greatest initial velocity ($5\ m/s$) the inflexion of the force is not reached, the energy is not completely dissipated by the HCPL and the maximum force generates a rebound. At first the thickness decreases linearly and then follows an inflexion in its variation. A sudden drop in thickness, due to great initial velocity or too heavy weight, would not allow the HCPL to totally dissipate the energy of an impact.

Case study: Impact of a human foot over a HCPL completely saturated with Newtonian liquid

All the theoretical models developed in XPHDL were focused on simple configurations, but the great number of possible applications (such as safety flooring for kids playground) would impose the use of diverse geometries with different boundary conditions, therefore, as a case study it is presented the impact of a human foot over a HCPL completely saturated with Newtonian liquid. The geometry of the 3D model which represents the human footprint is shown in Fig.8.

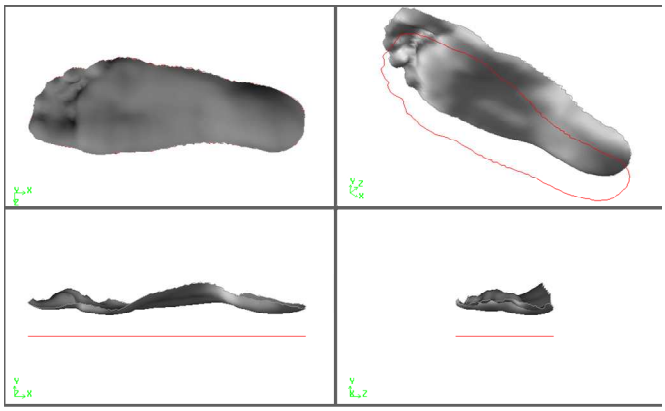

Fig. 8. Case study: 3D model of a human footprint.

The footprint with a mass of $50\ kg$ was given a normal (along y) initial velocity of $3.2\ m/s$. The HCPL has initial thickness of $50\ mm$, an initial compacticity of 0.03325 and is completely saturated with water of $0.001\ Pa \cdot s$ viscosity. The footprint has a length of $252\ mm$, is $90\ mm$ wide and is considered as rigid with respect to the HCPL, which is placed on a fixed rigid support. The system was considered open, with null pressure along boundaries and the footprint is constrained to the normal squeeze direction (along y). In Fig.9 are presented the contours of pressure [Pa] at a certain moment of the impact.

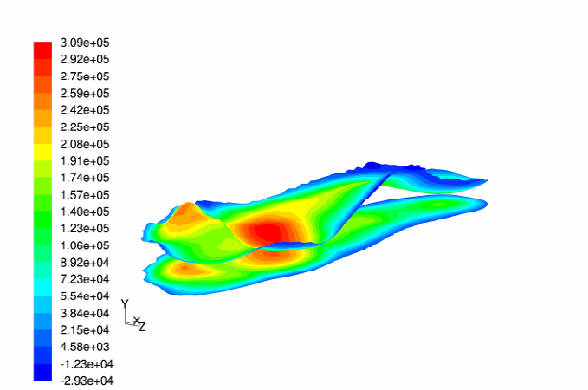

Fig. 9. Contours of pressure [Pa] on the footprint and on the fixed support generated by the impacted HCPL, at a certain moment.

The numerical results of the impact of a human foot over a HCPL saturated with water are presented in Fig.10. The dimensionless functions of force, velocity and thickness are represented with respect to the dimensionless time. The enlarged view offers a closer look at the first impact of the footprint.

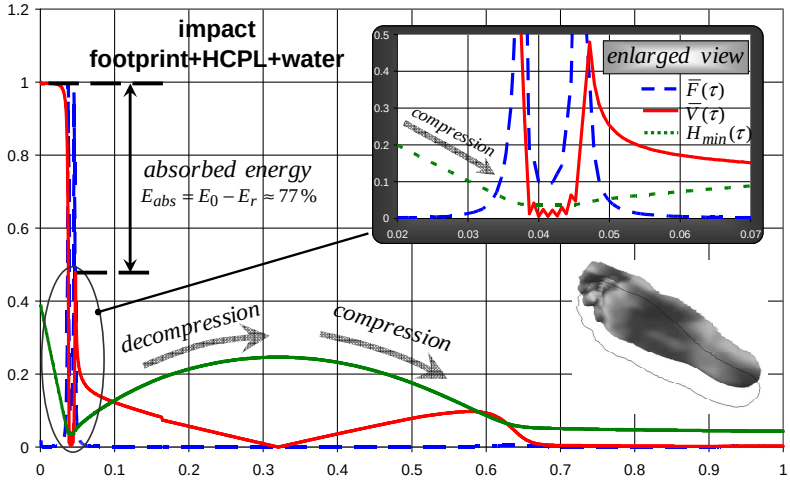

Fig. 10. Impact of a human foot over a HCPL completed saturated with water.

The difference between the initial velocity of the footprint and the maximum velocity reached after the rebound gives the energy absorbed by the HCPL:

$$E_{abs} = E_0 - E_r = \frac{MV_0^2}{2} - \frac{MV_r^2}{2} \tag{7}$$

For the studied case, the total energy of the impact $E_0 = 256\ J$ is absorbed by the HCPL after one rebound. In the first compression stage the energy absorbed is 197.48 J, due to the remaining energy, a decompression stage

follows and the remaining impact energy is completely dissipated in the second compression stage.

5. Conclusions

A numerical analysis of the HCPL completely saturated with Newtonian liquid squeezed at constant velocity / at constant loading / under impact was performed. The model was validated by experiment and by analytical model in the case of constant velocity and by analytical model in the case of impact, using the simple configuration disc+HCPL+liquid. A more complex geometry was analyzed as a case study of a 3D model: impact of a human foot on a HCPL completely saturated with water. The presented model extends the limits of XPHDL by taking into consideration the rebound of the impactor, if the energy of the impact is not totally dissipated, thus allowing the estimation of the absorbed energy by the HCPL.

6. Acknowledgments

I would like to express my gratitude to Professor Mircea Pascovici for teachings and advices regarding XPHDL.

Financial support for the work described in this paper was provided by National University Research Council (CNCSIS) under Grant IDEI 912.

7. Nomenclature

d – fibre diameter of HCPL; D – complex parameter of HCPL
E – energy; F – force; $\overline{F}$ – normalized force, $F / F_{\max}$
g – gravitational acceleration;
h – HCPL thickness in the contact area
H – dimensionless layer thickness, h / h_0
k – correction constant; M – mass
$\overline{M}$ – dimensionless mass, M / kg ; $\overline{p}$ – dimensionless momentum
R – disc radius; t – time; V – velocity
$\overline{V}$ – normalized velocity, $V / V_{\max}$;
$\overline{V_0}$ – dimensionless initial velocity, $V /(m / s)$

Greek letters

η – liquid viscosity; σ – HCPL compacticity
τ – dimensionless time, t / t_f ; ϕ – HCPL permeability

Subscripts/ Superscripts/ Abbreviations/ Acronyms

0 – initial; *abs* – absorbed; *compr* – compression;
ct – constant; *decompr* – compression; *f* – final
imp – impact; *m* – minimal; *r* – rebound
HCPL – highly compressible porous layer
XPHDL – ex-poro-hydrodynamic lubrication

REFERENCES

[1] *M. D. Pascovici*, Procedeu de pompare prrin dislocarea fluidului şi dispozitiv pentru realizarea acestuia, Procedure and device for pumping by fluid dislocation. Brevet de invenţie, 109469; 1994.

[2] *M. D. Pascovici*, Lubrication by Dislocation: A New Mechanism for Load Carrying Capacity. In: Proceedings of second World Tribology Congress, Vienna, 2001. p. 41 [paper on CD].

[3] *M. D. Pascovici, T. Cicone*, Squeeze-film of unconformal compliant and layered contacts. Tribology Int 2003; 36: 791-799.

[4] *M. D. Pascovici*, Lubrication Processes in highly compressible, porous layers. In: 16èmes Journées Francophones de Tribologie, JFT 2007, 22-23 May, Poitiers, France. Invited paper; 2009, [to be published].

[5] *M. D. Pascovici,* Lubrication of red blood cells in narrow capillaries. A heuristic approach. In:, Proceedings of second Vienna International Conference on Micro and Nano-technology, Viennano ’07, March 14-16, Austria, 2007. p.95-100 [on CD].

[6] *M. D. Pascovici, T. Cicone, V. Marian,* Squeeze process under impact, în highly compressible porous layers, imbibed with liquids. Tribology Int 2009, 42: 1433-1438.

[7] *M. D. Pascovici, C. S. Popescu, V. Marian,* Impact of a rigid sphere on a highly compressible layer imbibed with a newtonian liquid. J of Eng Trib, in press.

[8] *J. Feng, S. Weinbaum,* Lubrication theory in highly compressible porous media: the mechanics of skiing, from red cells to humans. J. Fluid Mech 2000; 422: 281-317.

[9] *Q. Wu, Y. Andreapoulos, S. Weinbaum,* From red cells to snowboarding: a new concept for a train track. Phys Rev Lett 2004;,93(19): 194501-1-4.

[10] *Y. Han, S. Weinbaum, J. A. E. Spaan, and H. Vink,* Large – deformation analysis of the elastic recoil of fiber layers in a Brinkman medium with application to the endothelial glycocalyx. J Fluid Mech 2006;554: 217-235.

[11] *P. Mirbod, Y. Andreopoulos, S. Weinbaum,* On the generation of lift forces in random soft porous media. J Fluid Mech 2009;619: 147-166.

[12] *S. Weinbaum, X. Zhang, Y. Han, H. Vink, S. C. Cowin,* Mechanotransduction and flow across the endothelial glycocalyx. PNAS 2003;100: 7988-7995.

[14] *C. W. McCutchen,* The frictional properties of animal joints. Wear 1962;5: 1-17.

[14] *C. S. Popescu, V. Marian, M. D. Pascovici,* Experimental and theoretical analysis of the permeability for highly compressible porous layers. J of the Balkan Tribological Association 2009; 15(1):86-92.

[15] *C. S. Popescu,* Dynamic permeability of highly compressible porous layers under squeeze at constant velocity and under impact, Tribology Int, DOI:10.1016/j.triboint.2010.10.030.

[16] *A. E. Scheidegger,* The physics of flow through porous media. 3rd ed. New York: University of Toronto Press; 1974.

[17] *C. K. Ghaddar,* On the permeability of unidirectional fibrous media. A parallel computational approach. Phys Fluids 1995;7(11): 2563-2586.

[18] Fluent 6.3 User’s Guide, Fluent Inc, 2006.